Hindawi
Journal of Chemistry
Volume 2020, Article ID 1710989, 10 pages
https://doi.org/10.1155/2020/1710989

Research Article

A Visible-NIR Responsive Dye-Sensitized Solar Cell Based on Diatom Frustules and Cosensitization of Photopigments from Diatom and Purple Bacteria

Xixiang Xiao,[1] Xiaobo Zhang,[1] Haiyang Su,[1] Shicheng Chen,[2] Zhihui He,[3] Chungui Zhao ,[1] and Suping Yang [1]

[1]*College of Chemical Engineering, Huaqiao University, Xiamen 361021, China*
[2]*Department of Microbiology and Molecular Genetics, Michigan State University, East Lansing, Michigan 48863, USA*
[3]*Hunan Changsha National Biological Industrial Base, Changsha 410331, China*

Correspondence should be addressed to Chungui Zhao; chungui@hqu.edu.cn and Suping Yang; 360825422@qq.com

Received 21 January 2020; Revised 1 March 2020; Accepted 4 March 2020; Published 24 April 2020

Academic Editor: Nenad Ignjatović

Diatoms exhibit high solar energy harvesting efficiency due to their remarkably organized, hierarchical micro/nanoporous, light-trapping, and scattering frustules. At present, few studies focus on cosensitization of natural near-infrared dye to expand the spectral response of dye-sensitized solar cells. In this study, the diatom frustule-TiO_2 (12 : 5) composite film was prepared and assembled it on the TiO_2 electrode. Compared to the single TiO_2 layer film, diatom frustule-TiO_2 (12 : 5) composite film sensitized by diatom's dye showed the conversion efficiency of 0.719%. To expand the light-harvesting response to near-infrared region spectra, the cosensitized dyes were used to fabricate the visible-near-infrared responsive dye-sensitized solar cells. The cosensitization diatom frustule-TiO_2 (12 : 5) composite film exhibited two distinct absorption bands in the near-infrared region and reached a higher conversion efficiency of 1.321%, which was approximately 1.4 or 1.7 folds higher than that of cosensitization double-TiO_2 film or single TiO_2 layer film, respectively, and approximately 3.7 or 1.7 folds higher than that of the single TiO_2 layer film sensitized by diatom dye or purple bacterial dye, respectively. The results showed that the combination between diatom frustule-TiO_2 with cosensitization natural dyes could significantly improve the photoelectric performance of visible-near-infrared responsive dye-sensitized solar cells.

1. Introduction

Dye-sensitized solar cells (DSSC) have attracted considerable attention due to their ease of fabrication, low production costs, and architectural and environmental compatibility compared to silicon-based solar cells [1–4]. Currently, the dyes used in DSSC mainly fous on synthetic dyes and some plant natural dyes. Synthetic dyes such as N719 and N3 ruthenium are capable of yielding higher conversion efficiencies [5–7]. However, their fabrication is complicated, and some are toxic [8]. Natural dyes are abundant, easily available, cost-effective, and eco-friendly [9, 10]; however, the conversion efficiency of DSSC was yet to be improved. In general, a challenge in DSSC is the expansion of absorbance range of photoactive layers. To the best of our knowledge, up to 50% of solar spectra are larger than 700 nm, which are located in the range of the infrared radiation [11]; however, the absorption maxima in most of the synthetic or natural dyes in DSSC are within 700 nm [10], and their conversion efficiency in the available DSSCs may be compromised due to limited sunlight absorption of dyes. Therefore, more interests are focused on exploring the near-infrared absorbance dyes or spectral complementary cosensitization dyes, such as synthesized FT89 NIR dye enhanced photocurrent conversion efficiency by 6% compared to N749 benchmark [12]; bacteriochlorophyll *c* (BChl *c*) from green sulfur bacterium showed a photocurrent conversion efficiency of 0.1% at 600–800 nm [13]. Cosensitizers

(N719, black dye, SQ1, NI5, and porphyrin) could enhance the photoelectric performance of DSSC [14–16]. However, few studies focus on natural NIR dye or cosensitized natural NIR dye.

The strategy for improving the structure and composition of TiO_2 electrodes is an additional effective approach to enhance the performance of DSSC, such as a double-layer TiO_2 film consisting of transparent nanocrystalline and microcrystalline light-scattering anatase particles was used for photocurrent enhancement of DSSC [17]. Mohammadpour and Janfaza coated nanofibrous as the scattering layer on the TiO_2 film, enhancing photocurrent by 11% [18]. These results showed that scattering double-layer electrodes exhibited a power performance. Novel structure, such as TiO_2 nanowires or nanotubes, was also used to enhance the performance of DSSC [19, 20].

Diatom frustule could be a promising photoelectric device [21–24]. Previous studies showed that diatom frustule-TiO_2 composites as the working electrode could enhance DSSC efficiency. Toster et al. coated frustules with titania nanoparticles to improve the conversion efficiency of DSSC [22]. Huang et al. made diatom frustule-TiO_2 composite electrodes with a multilayer structural design, enhancing efficiency by 38% [23]. In the above studies, sensitizers used in DSSC are N719 synthetic dyes. It remains unclear whether the diatom frustules could improve photoelectric performance of TiO_2 electrodes sensitized by natural dyes or other dyes.

Our previous study showed that pigment extracts from purple bacteria exhibited the maximal absorption at ~770 nm (bacteriochlorophyll *a*) in the NIR region and at 400~550 nm in the visible region, and diatom pigment extract exhibited the maximal absorption at ~660 nm (chlorophyll *a*) [25, 26]. The aim of this study was to design diatom frustule-TiO_2 composite and cosensitize it by two near-infrared spectral complementary natural dyes from purple bacteria and diatom with wide spectrum (400 nm~770 nm) in order to improve the photoelectric conversion efficiency of DSSC. This study showed that pigment extracts from purple bacteria exhibited the characteristic maximal absorption in the NIR region (at ~770 nm, bacteriochlorophyll *a*) and in the visible region (at 400~550 nm), and the pigment extract from the diatom exhibited the maximal absorption in the visible region (at ~660 nm, chlorophyll *a*). The absorption spectra of the three pigment mixtures displayed an expanding absorption region from Vis to NIR (400~500 nm, ~660 nm, and ~770 nm). The aim of this paper was to prepare diatom frustule-TiO_2 composite and cosensitize it by two near-infrared spectral complementary natural dyes from purple bacteria and diatom. The results showed that the combination utilization of diatom frustules and cosensitized dyes greatly enhanced the photoelectric performance of visible-NIR responsive DSSC. This work highlighted the trends in using the biomolecular photosensitizers with Vis-NIR absorbance or spectral complementary cosensitization characteristics for the dye-sensitized solar cell and also demonstrated that natural pigment extracts from diatom and purple bacteria and diatom frustules have the potential to be used as materials for fabricating low-cost and eco-friendly dye-sensitized solar cells.

2. Materials and Methods

2.1. Materials. Diatom NA56 came from Dongguan Minyi Biotechnology Company. Purple bacteria *Rhodopseudomonas palustris* strain CQV97 was cultured anaerobically in the modified Ormerod medium [26] at 30°C, 2500 lx.

2.2. Extraction of the Pigment and Diatom Frustules. Pigment was extracted from diatom NA56 following the method as described as follows. In brief, 10 g of wet cells was extracted in 100 mL of acetone and under ultrasonic treatment (pulse 4 s, stop 6 s, 400 W, 90 times) of ice bath for 15 min in dim light. Extract was fractioned by centrifuging, and the supernatant solvent was dried under nitrogen. The dried extract suspended in ethanol was the pigment extract of NA56. The pigment of purple bacteria CQV97 was extracted with an acetone/methanol mixture (7 : 2, V/V) as described previously [27]. In brief, 5 g of wet cells was extracted in 60 mL of the acetone/methanol mixture and under the conditions similar to those used for diatom. The dried extract suspended in ethanol was the pigment extract of CQV97. Pigment extracts were stored at −20°C under dark conditions.

The extract of frustules was based on Gell's methods [28]. Deal diatoms with hydrogen peroxide (30 wt%) and hydrochloric acid (2 mol·L^{-1}) mixture (V/V = 1 : 1) for 72 h under dark conditions in order to remove carbonates and organic matter. The pellet was rinsed with ethanol two times and widely washed with distilled water to get neutral pH. Diatom frustules were dried for 3 h at 130°C.

2.3. Preparation of the TiO_2 Film and Diatom Frustule-TiO_2 Film. A TiO_2 colloid was prepared as described previously [29]. Tetrabutyltitanate (10 mL) was rapidly added to distilled water (100 mL), and a white precipitate formed immediately. The precipitate was filtered using a glass frit and washed with distilled water. Under vigorous stirring, the filter cake was added to aqueous solution (150 mL) containing 1 mL nitric acid and 10 mL acetic acid at 80°C until the slurry became a translucent blue-white liquid. The blue-white liquid was autoclaved at 200°C for 12 h to form a milky, white slurry. The resultant slurry was concentrated to 25% of its original volume, and then PEG-20000 (0.80 g) and a few drops of the Triton X-100 emulsification reagent were added to form a TiO_2 colloid, labeled T_0. The TiO_2 colloid was coated on the fluorine-doped tin oxide-coated glass plate using a doctor scraping method followed by sintering at 450°C for 30 min in air. TiO_2 film was immersed in 50 mM $TiCl_4$ aqueous solution at 70°C for 30 min and sintered at 450°C for 30 min in air again. The film was labeled T, and the thickness and area of it were controlled to be about 8 μm and 0.1 cm^2, respectively.

The procedures used for the diatom frustule-TiO_2 colloid were similar to those for the TiO_2 colloid. 0.40 g, 0.80 g,

1.20 g, 1.60 g, and 0.80 g diatom frustules were added to distilled water (20 mL), respectively, and sonicated for 30 min. Subsequently, tetrabutyltitanate (2 mL) was rapidly added (except for the fifth group) to distilled water containing diatom frustules, respectively, and followed procedures were the same with preparation of TiO_2 colloid. The colloids were labeled F_1, F_2, F_3, F_4, and F_0 in turn. Then, T_0 (without diatom frustules), F_1, F_2, F_3, F_4, and F_0 (without TiO_2) colloids were individually coated on the T film. After sintering at 450°C for 30 min in air, double-layer films were obtained and labeled TT (cosensitization double TiO_2 film), TF1(diatom frustule-TiO_2 (4 : 5) composite film), TF2 (diatom frustule-TiO_2 (8 : 5) composite film), TF3 (diatom frustule-TiO_2 (12 : 5) composite film), TF4 (diatom frustule-TiO_2 (6 : 5) composite film), and TF0 (diatom frustules without the TiO_2 film) in sequence.

2.4. Dye-Sensitized TiO_2 Film and Diatom Frustule-TiO_2 Film

2.4.1. Different Concentrations of the Pigment Extract-Sensitized TiO_2 Film. The concentration of NA56 or CQV97 pigment extracts was determined by the amount of Chl *a* or BChl *a*, respectively. The single TiO_2 layer films (T) were placed in five concentrations of NA56 (with Chl *a* concentration of 19, 38, 155, 310, and 620 $\mu g \cdot mL^{-1}$) and CQV97 (with BChl *a* concentration of 9, 36, 144, 288, and 576 $\mu g \cdot mL^{-1}$) pigment extracts at 4°C for 24 h, respectively.

2.4.2. Cosensitization. The T films cosensitized by NA56 and CQV97 pigment extracts were prepared following two methods. (i) The cocktail process, in which the T films were immersed into the mixture of NA56 and CQV97 pigment extracts (V/V, 1 : 1, at the concentration optimized) at 4°C for 24 h. (ii) The step-by-step process, in which the T films were first immersed in the NA56 pigment extract for 0 h, 2 h, 6 h, 12 h, 18 h, 22 h, and 24 h, respectively, and subsequently transferred into the CQV97 pigment extract and incubated for 24 h, 22 h, 18 h, 12 h, 6 h, 2 h, and 0 h in sequence.

2.4.3. Diatom Frustule-TiO_2 Film Sensitized by the NA56 Pigment Extract. The TT, TF1, TF2, TF3, TF4, and TF0 films were immersed in the NA56 pigment extract at 4°C for 24 h. TF3 with a better photoelectric performance and its thickness were next optimized. Different amounts of the F_3 colloid were coated on the T film (8 μm) and sintered at 450°C for 30 min, and TF3 films were controlled with the thickness of 12 μm, 14 μm, 16 μm, and 18 μm, respectively. Subsequently, they were immersed in NA56 pigment extracts at 4°C for 24 h.

2.4.4. Diatom Frustule-TiO_2 Film Sensitized by Different Dyes. The TF3 Films were immersed in NA56 pigment extracts, CQV97 pigment extracts, cosensitizers (NA56 and CQV97 pigment extracts), and N719 (unique dye of DSSC based on diatom frustules reported previously) at 4°C for 24 h.

2.5. Fabrication of DSSC. The pigment-sensitized T and TF electrodes and Pt counter electrode were clipped together, and cyanoacrylate adhesive was used as sealant. The composition of the electrolyte was 0.1 M I_2, 0.1 M LiI, 0.6 M tetrabutylammonium iodide, and 0.5 M 4-tertbutylpyridine in acetonitrile.

2.6. Characterization and Measurement. The absorption spectra of pigment extracts and dye-sensitized electrodes were recorded from 300 to 900 nm using the UV-3200PCS spectrophotometer. The morphologies of diatom frustules and diatom frustule-TiO_2 composites were observed by a field emission scanning electron microscope (FESEM) (S-4800, HITACHI).

The photoelectric test of DSSC was performed by measuring photocurrent-photovoltage (I-V) characteristic curves at room temperature, white light of 100 $mW \cdot cm^{-2} \cdot t$ (AM1.5) irradiated from a solar simulator, and a CHI660D electrochemical measurement system. According to the I-V curves, the relevant parameters were measured, and the efficiency was calculated. The filling factor (FF) and conversion efficiency (η) of DSSC were calculated from the I-V curve, and equation $FF = P_{opt}/(I_{sc} \times V_{oc}) = (I_{opt} \times V_{opt})/(I_{sc} \times V_{oc})$, $\eta = P_{opt}/P_{in} = (FF \times I_{sc} \times V_{oc})/P_{in}$. In the above equation, I_{sc} represents the short-circuit current, I_{opt} represents the optimal photocurrent, V_{oc} represents the open-circuit voltage, V_{opt} represents the optimal photovoltage, P_{opt} represents the optimal output power of the battery, and P_{in} represents the sunlight input power.

3. Results and Discussion

3.1. Characterization of Pigment Extracts. Figure 1(a) shows the absorption spectra of NA56 and CQV97 pigment extracts dissolved in ethanol. NA56 pigment extract mainly consisting of Ch *a* and Car exhibits absorption peaks in the visible region at approximately 410 nm (Ch *a*), 666 nm (Ch *a*), and 450 nm (Car). CQV97 pigment extract mainly consisting of BCh *a* and Car shows absorption peaks in the UV-NIR region at approximately 368 nm (BCh *a*), 598 nm (BCh *a*), 774 nm (BCh *a*), and 475 nm (Car). Cosensitizer of NA56 and CQV97 pigment extracts exhibits a wider spectral response range than the individual pigment extract.

Figure 1(b) shows the absorption spectra of pigments adsorbed on the TiO_2 film. Compared with Figure 1(a), the characteristic absorption peaks in Figure 1(b) were red-shifted. The absorption spectra of the cosensitizer on the TiO_2 film were expanded within the Vis to NIR region and displayed both characteristic absorption peaks of the pigment extract from NA56 and CQV97. This might be an important reasonable reason for improving photoelectric properties of the cosensitizer on the TiO_2 film.

3.2. The Photoelectric Performance of Different Concentrations of the Pigment Extract-Sensitized TiO_2 Film. As shown in Figures 2(a) and 2(b), η and I_{sc} increase from 19 to 155 $\mu g \cdot mL^{-1}$ of Chl *a* and 9 to 144 $\mu g \cdot mL^{-1}$ of BChl *a*, respectively, but decrease with further increase in

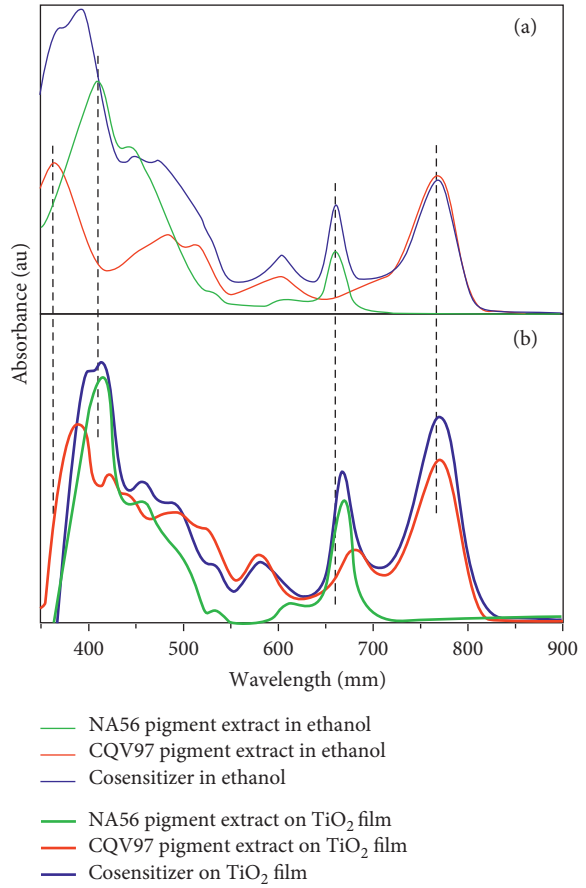

Figure 1: UV-Vis absorption spectra of NA56 and CQV97 pigment extracts, and the cosensitizer of them in ethanol (a) and on the TiO_2 film (b).

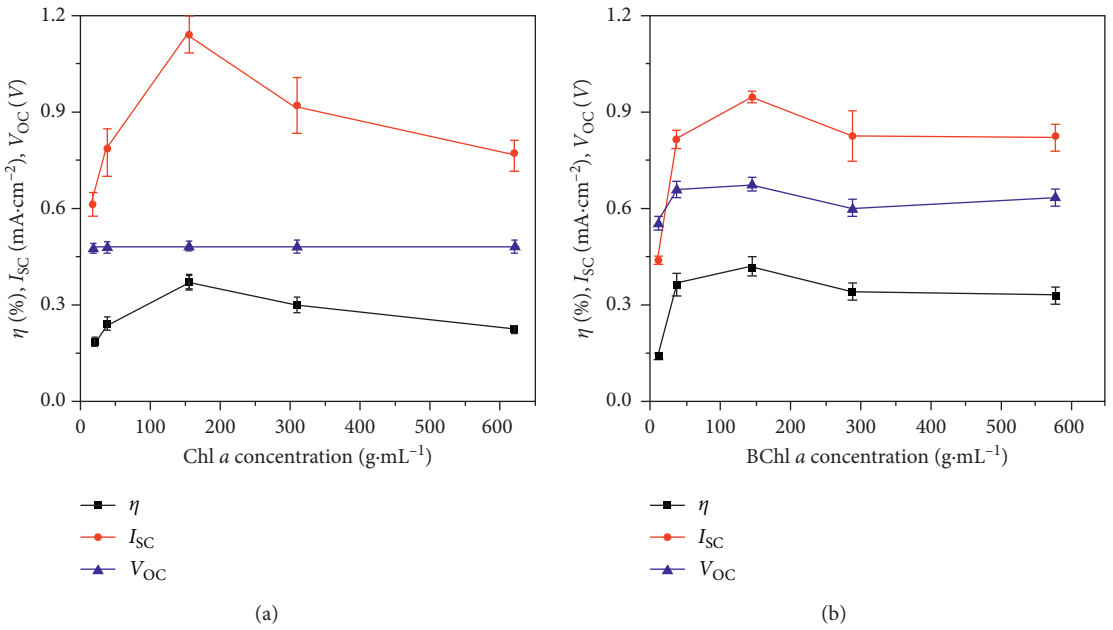

Figure 2: Photoelectric parameters of different concentrations of NA56 (a) and CQV97 (b) pigment extract-sensitized solar cells (standard deviation is the calculate values based on the measurements of three parallel solar cells).

concentration. Dye in the film will build up with increasing concentration, and an increase in η and I_{sc} would be expected. Dye aggregation, however, becomes more serious in higher concentration, which may lead to intermolecular quenching of photo-excited states or molecules residing in the system that are not functionally attached to the TiO_2 surface, causing the decrease of η and I_{sc} [30]. And V_{oc} fluctuates slightly with the change of concentration. The highest η and I_{sc} values of NA56 and CQV97 pigment extracts are 0.368%, 1.139 mA·cm^{-2} and 0.417%, 0.950 mA·cm^{-2} at the concentration 155 μg·mL^{-1} (Chl *a*) and 144 μg·mL^{-1} (BChl *a*), respectively.

3.3. Cosensitization of NA56 and CQV97 Pigment Extracts. The photovoltaic parameters of the cosensitizer sensitized by the *T* film are shown in Table 1. A slight increment of conversion efficiency (0.432%) is observed in the pigment extract mixture-cosensitized DSSC compared to individual pigment extract-sensitized DSSC (0.420%, 0.372%).

Remarkably, the photoelectric performance is greatly enhanced by the cosensitization through stepwise procedure. The maximum values of η and I_{sc} reach up to 0.795% and 1.913 mA·cm^{-2} when T films are immersed in the NA56 pigment extract for 12 h and then in the CQV97 pigment extract for 12 h. η exceeds NA56 and CQV97 extract-sensitized DSSC (0.372%, 0.420%) by 114% and 89%, respectively. Such increase is possibly attributed to higher light-harvesting capacities of the cosensitizer, which is in agreement with the UV-Vis spectra (see Figure 1) of individual pigment extracts and cosensitizer. After absorption on the TiO_2 film, both individual pigment extracts and cosensitizer show characteristic absorption spectra with redshift when compared to their absorption spectrum of dye solution, and cosensitizer demonstrates absorption bands in the visible region at ~400 nm and ~670 nm and the NIR region at ~770 nm, with a highly broadened spectral response range. Furthermore, cosensitizer exhibits a great potential to enhance light-harvesting capacities if compared to individual dyes. As shown in Table 1, DSSC cosensitized by stepwise procedure are more efficient than the mixture-sensitized DSSC. When NA56 and CQV97 extracts are mixed, unfavorable intermolecular interaction such as dye aggregation could occur which restricts the utilization of original properties of individual dyes for efficient photoenergy conversion process [31]. Stepwise cosensitization could retard the charge recombination and decrease aggregation of the dye absorbed on the TiO_2 film to further improve the device performance [32].

3.4. The Photoelectric Performance of the NA56 Pigment Extract-Sensitized Diatom Frustule-TiO_2 Film. As shown in Table 2, DSSC with the double-layer film are more efficient (except for TF0) than the single layer. The conversion efficiency of the NA56 pigment extract-sensitized TT, TF1, TF2, TF3, and TF4 film is 0.520%, 0.641%, 0.706%, 0.719%, and 0.522% in sequence, exceeding that sensitized *T* film by 41%, 74%, 92%, 95%, and 42%, respectively. The photocurrent of DSSC firstly increases and then decreases with the increasing diatom frustules mass ratio of the second layer (Figure 3); a similar trend is seen in their conversion efficiency. However, under the same conditions, V_{oc} slightly changes. The maximum values of η and I_{sc} reach up to 0.719% (exceeding *T* and TT films by 95% and 38%) and 2.006 mA·cm^{-2} (exceeding *T* and TT films by 76% and 41%) when the mass ratio of diatom frustules/TiO_2 of the second layer is 12 : 5 (TF3 film). The improvement for the cell incorporating diatom frustules is possibly attributed to enhanced light scattering and trapping. When light strikes diatom frustules, the pores cause multiple reflections thereby increasing the probability for photons to be absorbed by the dye and promoting injection into the semiconductor [22, 23]. As shown in Figure 4, after the NA56 pigment extract is absorbed on TiO_2 and frustule-TiO_2 film, both of them show absorption spectra with redshift as compared to that of dye solution. And the spectral response range on the frustule-TiO_2 film is wider than that on the TiO_2 film, which may be a reason why the diatom frustules incorporated into TiO_2 improved the photoelectric performance of DSSC.

Diatom frustules consist of two halves with many small holes on their surface, approximately 5 μm in width and 20 μm in length (Figure 5(a)). The small holes of the external surface with diameter of approximately 200 nm (Figure 5(b)) and internal surface of frustules (Figure 5(c)) have a honeycomb structure with smaller holes (with diameter of approximately 50 nm). The results above were basically consistent with the previous study [33]. The SEM images (Figures 5(d) and 5(e)) of diatom frustule-TiO_2 materials show that TiO_2 nanoparticles successfully coated the surface of diatom frustules, and the diameter of TiO_2 particles is about 20 nm.

TF3 thickness is optimized by attaching the second layer diatom frustule-TiO_2 film thickness (the first layer is T film with 8 μm thickness). The correlation between thickness and photoelectric performance parameters is shown in Figure 6 η and I_{sc} increase within the TF3 film thickness range between 12 and 14 μm but decrease with further increase in thickness. The charge recombination between electrons injected from the excited dye to the conduction band of TiO_2 and the I3 ions in the electrolyte will, however, become more serious in thicker films, which leads to the decrease of η and I_{sc} [34]. However, decreased V_{oc} is attributed to the charge recombination and mass transport limitations in the thicker film.

3.5. The Photoelectric Performance of Different Dye-Sensitized TT and TF3 Film. The above results show that diatom frustules incorporated into TiO_2 enhanced the photoelectric performance of the NA56 pigment extract-sensitized solar cell. Herein, to test whether the frustules can improve photoelectric performance of DSSC sensitized by other dyes, we further investigate the photovoltaic parameters of the CQV97 pigment extract, cosensitizer (NA56 and CQV97 pigment extracts), and N719-sensitized TT and TF3 films. As shown in Table 3, CQV97 pigment extract, cosensitizer (NA56 and CQV97 pigment extracts), and N719-sensitized TF3 films show conversion efficiency of 0.976%, 1.321%, and

Table 1: Photovoltaic parameters[a] of cosensitizer sensitized by T film electrodes (3 samples in each group).

Duration of dye loading	V_{OC} (V)	I_{SC} (mA·cm^{-2})	FF	η (%)
(NA56 + CQV97) (24 h)	0.607 ± 0.018	1.199 ± 0.120	0.610 ± 0.023	0.432 ± 0.028
NA56(0 h) + CQV97(24 h)	0.680 ± 0.006	0.952 ± 0.020	0.653 ± 0.054	0.420 ± 0.030
NA56(2 h) + CQV97(22 h)	0.698 ± 0.005	1.382 ± 0.022	0.703 ± 0.034	0.680 ± 0.048
NA56(6 h) + CQV97(18 h)	0.627 ± 0.005	1.694 ± 0.140	0.613 ± 0.011	0.655 ± 0.052
NA56(12 h) + CQV97(12 h)	0.654 ± 0.005	1.913 ± 0.143	0.639 ± 0.032	0.795 ± 0.031
NA56(18 h) + CQV97(6 h)	0.594 ± 0.013	1.844 ± 0.140	0.661 ± 0.011	0.725 ± 0.070
NA56(22 h) + CQV97(2 h)	0.548 ± 0.006	1.603 ± 0.034	0.684 ± 0.018	0.600 ± 0.034
NA56(24 h) + CQV97(0 h)	0.484 ± 0.005	1.140 ± 0.050	0.670 ± 0.025	0.372 ± 0.020

[a]Cell performance as reported is the average of four devices. V_{OC}: open-circuit voltage. I_{SC}: short-circuit current. FF: filling factor of DSSC. η: conversion efficiency of DSSC.

Table 2: Photovoltaic parameters[b] of NA56 pigment extract-sensitized diatom frustule-TiO_2 film electrodes (4 samples in each group).

Sample	Frustules/TiO_2 mass ratio of second layer	V_{OC} (V)	I_{SC} (mA·cm^{-2})	FF	η (%)
T	/[c]	0.484 ± 0.007	1.139 ± 0.055	0.670 ± 0.023	0.368 ± 0.021
TT	0 : 1	0.485 ± 0.005	1.426 ± 0.101	0.748 ± 0.009	0.520 ± 0.038
TF1	4 : 5	0.561 ± 0.050	1.670 ± 0.121	0.695 ± 0.043	0.641 ± 0.035
TF2	8 : 5	0.578 ± 0.016	1.789 ± 0.120	0.693 ± 0.016	0.706 ± 0.044
TF3	12 : 5	0.505 ± 0.008	2.006 ± 0.100	0.712 ± 0.010	0.719 ± 0.035
TF4	16 : 5	0.517 ± 0.006	1.388 ± 0.167	0.726 ± 0.015	0.522 ± 0.068
TF0	1 : 0	0.503 ± 0.007	0.848 ± 0.055	0.764 ± 0.031	0.326 ± 0.019

[b]Cell performance as reported is the average of four devices, and "/" represents no second layer. T: single TiO_2 layer film. TT: cosensitization double TiO_2 film. TF1: diatom frustule-TiO_2 (4 : 5) composite film. TF2: diatom frustule-TiO_2 (8 : 5) composite film. TF3: diatom frustule-TiO_2 (12 : 5) composite film. TF4: diatom frustule-TiO_2 (6 : 5) composite film. TF0: diatom frustules without the TiO_2 film. V_{OC}: open-circuit voltage. I_{SC}: short-circuit current. FF: filling factor of DSSC. η: conversion efficiency of DSSC. (4 samples in each group).

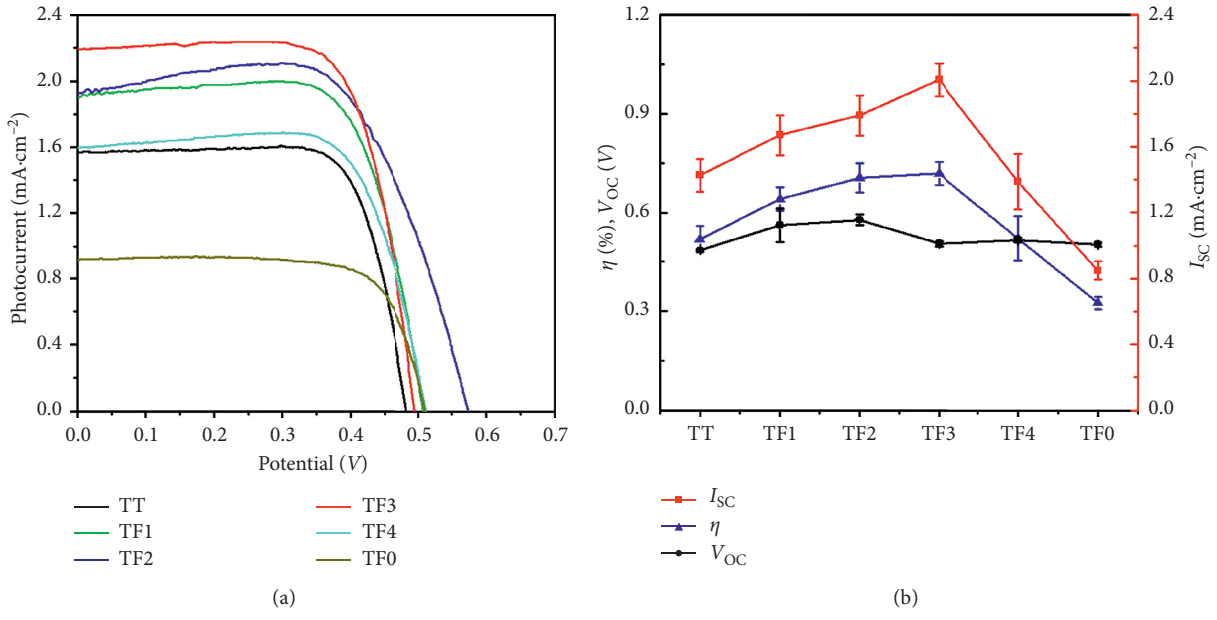

Figure 3: (a) I-V curves and (b) photoelectric parameters of TT, TF1, TF2, TF3, TF4, and TF0 film electrodes (standard deviation is stemmed from Table 2).

5.844%, enhancing efficiency by 42%, 32%, and 34% compared with that of the sensitized TT film, demonstrating diatom frustule-TiO_2 composites made in this work possibly improve photoelectric performance of solar cells sensitized by other dyes. This result was basically consistent with the previous study [23]. The conversion efficiency of cosensitizer (NA56 and CQV97 pigment extracts) sensitized by the TF3 film reaches up to 1.321%, exceeding that (0.998%, 0.520%, and 0.687%) of cosensitizer and individual dye-sensitized TT film by 32%, 154%, and 92%, respectively; furthermore, it enhances efficiency by 259% and 217% when compared with that (0.368% and 0.417%) of the individual dye-sensitized T film, respectively. It is more efficient than most of the reported chlorophyll- and carotenoid-sensitized solar cells.

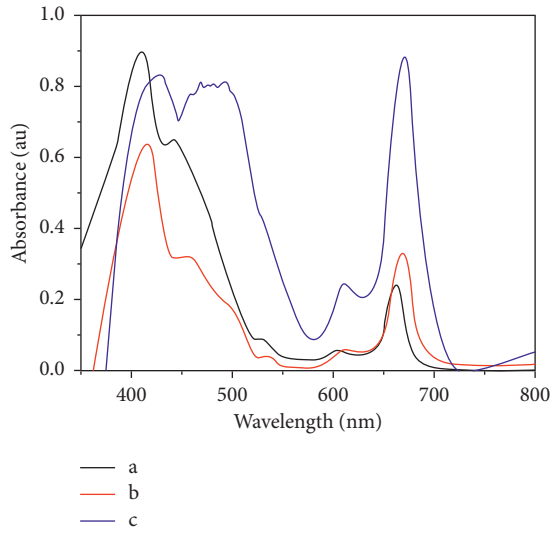

Figure 4: UV-Vis absorption spectra of the NA56 pigment extract (a) in ethanol, (b) on TiO_2 film, and (c) on diatom frustule-TiO_2 (TF3) film.

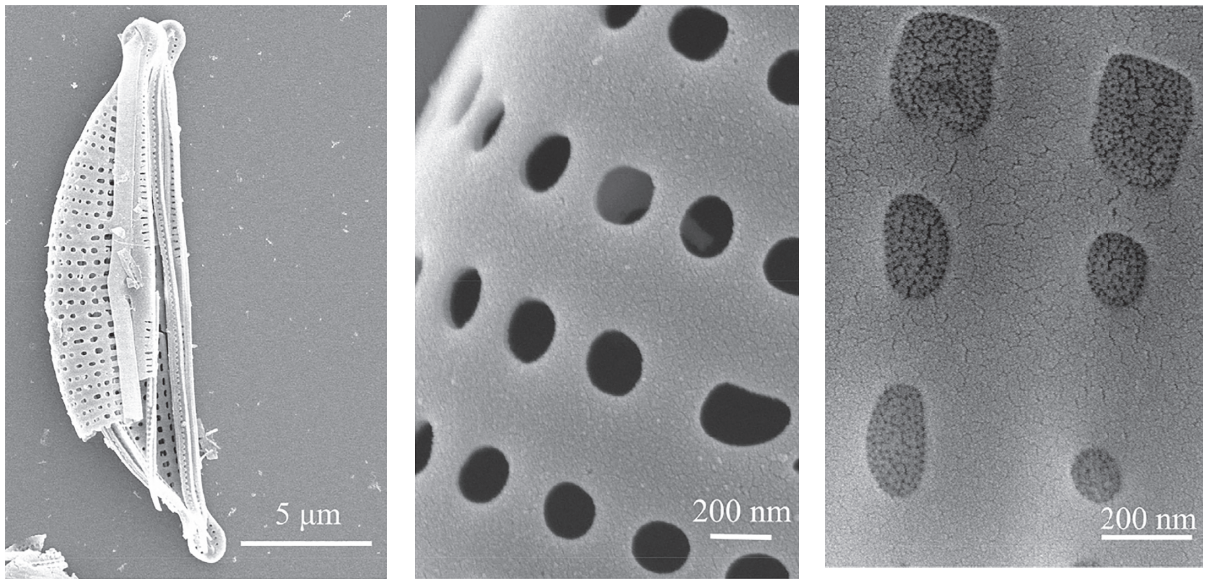

(a) (b) (c)

Figure 5: Continued.

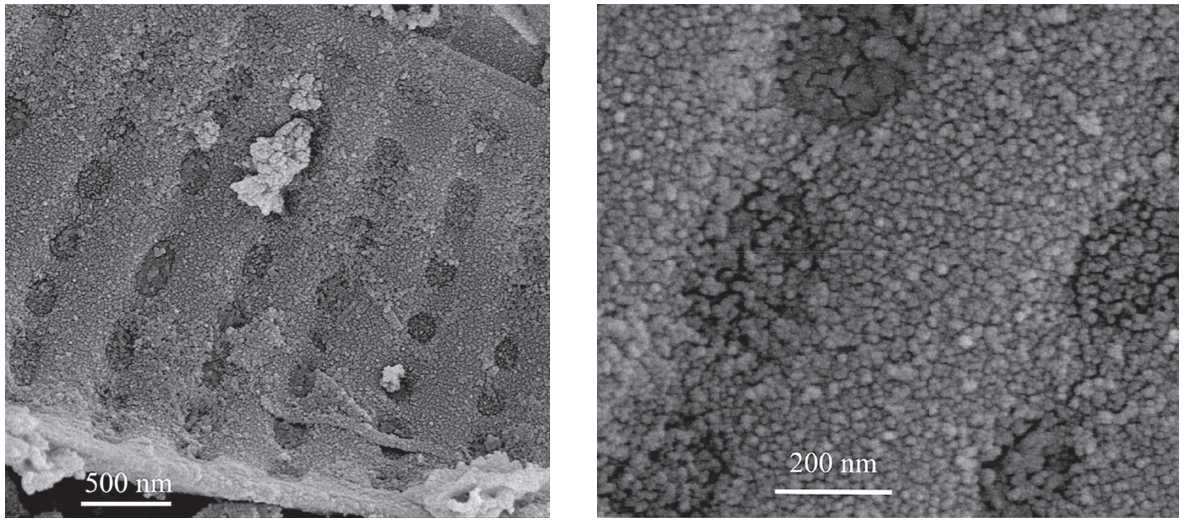

(d) (e)

Figure 5: SEM images of (a) diatom frustules, (b) the external surface of diatom frustules, (c) the internal surface of diatom frustules, and (d) and (e) diatom frustule-TiO_2.

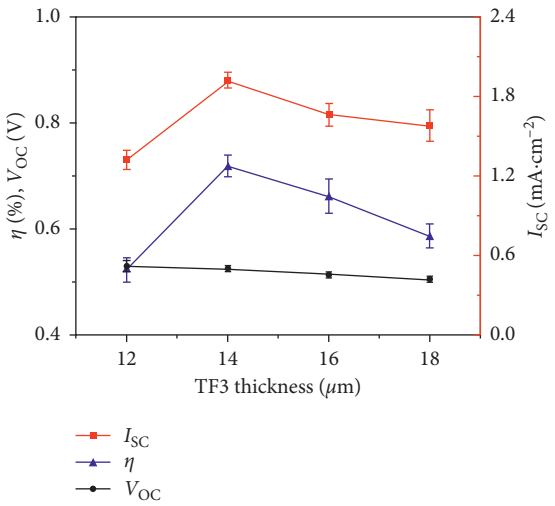

Figure 6: Photoelectric parameters of the TF3 film with different thicknesses (standard deviation is the calculate values based on the measurements of four parallel solar cells).

Table 3: Photovoltaic parameters[d] of dye-sensitized TT and TF3 film electrodes (3 samples in each group).

Film	Dyes	V_{OC} (V)	I_{SC} (mA·cm^{-2})	FF	η (%)
TT	CQV97 pigment extract	0.685 ± 0.035	1.330 ± 0.197	0.752 ± 0.035	0.687 ± 0.032
TT	(NA56 + CQV97) pigment extracts	0.634 ± 0.017	2.440 ± 0.122	0.645 ± 0.016	0.998 ± 0.042
TT	N719	0.790 ± 0.020	7.568 ± 0.218	0.703 ± 0.024	4.368 ± 0.129
TF3	CQV97 pigment extracts	0.736 ± 0.026	1.621 ± 0.321	0.774 ± 0.020	0.976 ± 0.022
TF3	(NA5 + CQV97) pigment extracts	0.664 ± 0.024	3.122 ± 0.150	0.635 ± 0.019	1.321 ± 0.096
TF3	N719	0.793 ± 0.016	10.740 ± 0.516	0.674 ± 0.033	5.844 ± 0.126

[d]Cell performance as reported is the average of four devices. TT: cosensitization double TiO_2 film. TF3: diatom frustule-TiO_2 composite (12 : 5) film. V_{OC}: open-circuit voltage. I_{SC}: short-circuit current. FF: filling factor of DSSC. η: conversion efficiency of DSSC.

Our results further demonstrated that combining cosensitizer with TiO_2 electrode incorporating diatom frustules greatly improved the photoelectric performance of DSSC.

4. Conclusion

In conclusion, our results showed that cosensitizer- (NA56 and CQV97 pigment extracts-) sensitized TiO_2 film exhibited absorption bands in the visible region at ~400 nm and ~670 nm and the NIR region at ~770 nm, expanding absorption spectra of individual dyes and yielding conversion efficiency of 0.795%, exceeding that of NA56 and CQV97 pigment extract-sensitized TiO_2 film by 114% and 90%, respectively. The NA56 pigment extract, CQV97 pigment extract, cosensitizer, and N719-sensitized solar cells incorporating diatom frustules (TF3 films) enhanced efficiency by 38%, 42%, 32%, and 34% compared with that of sensitized TT films, respectively. The conversion efficiency was further promoted (up to 1.321%) when a cosensitizer-sensitized TF3 film was created. It was more efficient than most of the available chlorophyll- and carotenoid-sensitized solar cells. Pigments of diatom and purple bacteria are easily extracted and eco-friendly. Diatom frustule is a structure designed by nature with the ability of trapping and scattering light. Apparently, the above results show that natural pigment extracts of diatom and purple bacteria and diatom frustules have the potential to be used as materials for fabricating low-cost and eco-friendly dye-sensitized solar cells.

Data Availability

The data used to support the findings of this study are enclosed within the article. Additional data are accessible from the corresponding author upon request.

Conflicts of Interest

The authors declare that there are no conflicts of interest regarding the publication of this paper.

Acknowledgments

The authors acknowledge the financial support by the National Natural Science Foundation of China (no. 31270106), National Marine Public Industry Research (no. 201505026), the Natural Science Foundation of Fujian Province (no. 2018J0149), and Subsidized Project for Cultivating Postgraduates' Innovative Ability in Scientific Research of Huaqiao University.

References

[1] M. Hosseinnezhad, M. Ghahari, H. Shaki, and J. Movahedi, "Investigation of DSSCs performance: the effect of 1, 8-naphthalimide dyes and Na-doped TiO_2," *Progress in Color, Colorants and Coatings*, vol. 13, pp. 177–185, 2020.

[2] Z. Parsa, P. Tahay, and N. Safari, "Co-sensitization of porphyrin and metal-free dye for panchromatic dye-sensitized solar cells," *Journal of the Iranian Chemical Society*, vol. 17, no. 2, pp. 453–459, 2020.

[3] T. Y. Kim, N. J. Jeon, H. Y. Jung, J. H. Kim, and S. Y. Cho, "Adsorption and photovoltaic properties of lac-color on TiO_2 for dye-sensitized solar cells," *Journal of Nanoscience and Nanotechnology*, vol. 20, pp. 1989–1992, 2020.

[4] M. Raïssi, Y. Pellegrin, F.-X. Lefevre et al., "Digital printing of efficient dye-sensitized solar cells (DSSCs)," *Solar Energy*, vol. 199, pp. 92–99, 2020.

[5] S. Mathew, A. Yella, P. Gao et al., "Dye-sensitized solar cells with 13% efficiency achieved through the molecular engineering of porphyrin sensitizers," *Nature Chemistry*, vol. 6, no. 3, pp. 242–247, 2014.

[6] F. Sauvage, J.-D. Decoppet, M. Zhang et al., "Effect of sensitizer adsorption temperature on the performance of dye-sensitized solar cells," *Journal of the American Chemical Society*, vol. 133, no. 24, pp. 9304–9310, 2011.

[7] A. Yella, H.-W. Lee, H. N. Tsao et al., "Porphyrin-sensitized solar cells with cobalt (II/III)-based redox electrolyte exceed 12 percent efficiency," *Science*, vol. 334, no. 6056, pp. 629–634, 2011.

[8] G. Calogero, A. Bartolotta, G. D. Marco, A. D. Carlo, and F. Bonaccorso, "Cheminform abstract: vegetable-based dye-sensitized solar cells," *Chemical Society Reviews*, vol. 46, no. 29, pp. 3244–3294, 2015.

[9] H. A. Maddah, V. Berry, and S. K. Behura, "Biomolecular photosensitizers for dye-sensitized solar cells: recent developments and critical insights," *Renewable and Sustainable Energy Reviews*, vol. 121, Article ID 109678, 2020.

[10] M. Shahid, S. Shahid-Ul-Islam, and F. Mohammad, "Recent advancements in natural dye applications: a review," *Journal of Cleaner Production*, vol. 53, pp. 310–331, 2013.

[11] B. Basheer, D. Mathew, B. K. George, and C. P. R. Nair, "An overview on the spectrum of sensitizers: the heart of dye sensitized solar cells," *Solar Energy*, vol. 108, pp. 479–507, 2014.

[12] T. Funaki, H. Funakoshi, O. Kitao et al., "Cyclometalated ruthenium (II) complexes as near-IR sensitizers for high efficiency dye-sensitized solar cells," *Angewandte Chemie*, vol. 124, no. 30, pp. 7646–7649, 2012.

[13] L.-K. Tsui, J. Huang, M. Sabat, and G. Zangari, "Visible light sensitization of TiO2 nanotubes by bacteriochlorophyll-C dyes for photoelectrochemical solar cells," *ACS Sustainable Chemistry & Engineering*, vol. 2, no. 9, pp. 2097–2101, 2014.

[14] S. Gao, R. Q. Fan, X. M. Wang et al., "Advanced CdII complexes as high efficiency co-sensitizers for enhanced dye-sensitized solar cell performance," *Dalton Transactions*, vol. 44, no. 41, pp. 18187–18195, 2015.

[15] N. Shibayama, H. Ozawa, M. Abe, Y. Ooyama, and H. Arakawa, "A new cosensitization method using the lewis acid sites of a TiO_2 photoelectrode for dye-sensitized solar cells," *Chemical Communications*, vol. 50, no. 48, pp. 6398–6401, 2014.

[16] H.-P. Wu, Z.-W. Ou, T.-Y. Pan et al., "Molecular engineering of cocktail co-sensitization for efficient panchromatic porphyrin-sensitized solar cells," *Energy & Environmental Science*, vol. 5, no. 12, pp. 9843–9848, 2012.

[17] A. M. Bakhshayesh, "Light scattering management of dye-sensitized solar cells based on double-layered photoanodes aided by uniform TiO_2 aggregates," *Materials Research Bulletin*, vol. 73, pp. 268–275, 2016.

[18] R. Mohammadpour and S. Janfaza, "Efficient nanostructured biophotovoltaic cell based on bacteriorhodopsin as biophotosensitizer," *ACS Sustainable Chemistry & Engineering*, vol. 3, no. 5, pp. 809–813, 2015.

[19] G. K. Mor, K. Shankar, M. Paulose, O. K. Varghese, and C. A. Grimes, "Use of highly-ordered TiO_2 nanotube arrays in dye-sensitized solar cells," *Nano Letters*, vol. 6, no. 2, pp. 215–218, 2006.

[20] J. Xiao, P. Li, and X. Wen, "Alkali-corrosion synthesis and excellent DSSC performance of novel jujube-like hierarchical TiO_2 microspheres," *Nanotechnology*, vol. 29, no. 17, Article ID 175603, 2018.

[21] R. Gordon, D. Losic, M. A. Tiffany, S. S. Nagy, and F. A. S. Sterrenburg, "The glass menagerie: diatoms for novel applications in nanotechnology," *Trends in Biotechnology*, vol. 27, no. 2, pp. 116–127, 2009.

[22] J. Toster, K. S. Iyer, W. Xiang, F. Rosei, L. Spiccia, and C. L. Raston, "Diatom frustules as light traps enhance DSSC efficiency," *Nanoscale*, vol. 5, no. 3, pp. 873–876, 2013.

[23] D.-R. Huang, Y.-J. Jiang, R.-L. Liou, C.-H. Chen, Y.-A. Chen, and C.-H. Tsai, "Enhancing the efficiency of dye-sensitized solar cells by adding diatom frustules into TiO_2 working electrodes," *Applied Surface Science*, vol. 347, pp. 64–72, 2015.

[24] T. M. W. J. Bandara, M. Furlani, I. Albinsson, A. Wulff, and B.-E. Mellander, "Diatom frustules enhancing the efficiency of gel polymer electrolyte based dye-sensitized solar cells with multilayer photoelectrodes," *Nanoscale Advances*, vol. 2, no. 1, pp. 199–209, 2020.

[25] Q. Fu, C. Zhao, S. Yang, and J. Wu, "The photoelectric performance of dye-sensitized solar cells fabricated by assembling pigment-protein complexes of purple bacteria on nanocrystalline photoelectrode," *Materials Letters*, vol. 129, pp. 195–197, 2014.

[26] C. Zhao, H. Yue, Q. Cheng, S. Chen, and S. Yang, "What caused the formation of the absorption maximum at 421 nmin Vivospectra of *Rhodopseudomonas palustris*," *Photochemistry and Photobiology*, vol. 90, no. 6, pp. 1287–1292, 2014.

[27] M. Q. Zhuo, C. G. Zhao, Q. Cheng, S. P. Yang, and Y. B. Qu, "Fingerprinting analysis of photopigments in purple bacteria," *Acta Microbiologica Sinica*, vol. 52, no. 6, pp. 760–768, 2012.

[28] P. A. Gell, "The development of a diatom database for inferring lake salinity, western Victoria, Australia: towards a quantitative approach for reconstructing past climates," *Australian Journal of Botany*, vol. 45, no. 3, pp. 389–423, 1997.

[29] J. Wu, S. Hao, Z. Lan et al., "An all-solid-state dye-sensitized solar cell-based poly (N-alkyl-4-vinyl-pyridine iodide) electrolyte with efficiency of 5.64%," *Journal of the American Chemical Society*, vol. 130, no. 35, pp. 11568-11569, 2008.

[30] S. Ito, H. Miura, S. Uchida et al., "High-conversion-efficiency organic dye-sensitized solar cells with a novel indoline dye," *Chemical Communications*, vol. 44, no. 41, pp. 5194–5196, 2008.

[31] N. T. R. N. Kumara, P. Ekanayake, A. Lim et al., "Layered co-sensitization for enhancement of conversion efficiency of natural dye sensitized solar cells," *Journal of Alloys and Compounds*, vol. 581, pp. 186–191, 2013.

[32] L. Hui, Y. Z. Wu, Z. Y. Geng, and J. C. Liu, "Co-sensitization of benzoxadiazole based D-A-π-A featured sensitizers: compensating light-harvesting and retarding charge recombination," *Journal of Materials Chemistry A*, vol. 2, no. 35, pp. 14649–14657, 2014.

[33] S. Yamanaka, R. Yano, H. Usami, and N. Hayashida, "Optical properties of diatom silica frustule with special reference to blue light," *Journal of Applied Physics*, vol. 103, no. 7, pp. 074701–074706, 2008.

[34] Z. S. Wang, H. Kawauchi, T. Kashima, and H. Arakawa, "Significant influence of TiO_2 photoelectrode morphology on the energy conversion efficiency of N719 dye-sensitized solar cell," *Coordination Chemistry Reviews*, vol. 248, no. 13-14, pp. 1381–1389, 2004.